DOI: https://doi.org/10.14311/TPFM.2025.028

FEATURES OF THE VORTEX STRUCTURES IN CAVITIES OF DIFFERENT DEPTH

N. Rozumnuk[1], O. Baskova[1, 2], V. Kravchenko[3], G. Baskova[4]

[1] Department of the Hydrobionics and Boundary Layer Control, Institute of Hydromechanics National Academy of Sciences of Ukraine, Marii Kapnist str., 8/4, 03057 Kyiv, Ukraine

[2] Educational and Research Institute of Nuclear and Heat Power Engineering, National Technical University of Ukraine "Igor Sikorsky Kyiv Polytechnic Institute", Beresteiskyi ave., 37, 03056 Kyiv, Ukraine

[3] Department of Physics and Mathematics, Kruty Heroes Military Institute of Telecommunications and Information Technology, 45/1 Knyazum Ostrozkih Street, Kyiv, 01011, Ukraine

4 Department of Descriptive Geometry, Engineering and Computer Graphics, National Technical University of Ukraine "Igor Sikorsky Kyiv Polytechnic Institute", Beresteiskyi ave., 37, 03056 Kyiv, Ukraine

Abstract

The vortex flow features in and behind three-dimensional cavities with rectangular cross sections were studied based on direct numerical simulations. The Reynolds numbers range of $Re_w \approx 5000 \ldots 10000$ and non-isothermal flow were considered. The results obtained showed a significant dependence of vortical flow on the cavity depth. The cavity flow variations in the transverse direction were obtained that can propagate into the external flow and induce earlier development of downstream instability, while the presence of a cavity does not change essentially the integral characteristics of the channel flow under the considered conditions.

Keywords: rectangular cavity, vortex structure, flow stability

1 Introduction

Vortex management has been and remains one of the key issues of hydrodynamics for many years, not least due to the prospects of practical use of research results. The type of equipment where a vortex flow is expected to occur determines the desired characteristics of such flow. Thus, the transport industry is focused on solving the problem of reducing hydraulic resistance, while for power equipment the main task is intensification of heat transfer. Sometimes the requirements for flow characteristics in equipment elements can be mutually exclusive. In this case, it is necessary to solve a more complex and difficult task of creating a vortex structure with such characteristics, at which it is possible to achieve an optimal operating mode. To date, vortex generators in the form of ledges and cavities of various shapes on the streamlined surface have become widespread. In particular, widely studied are cavities with a rectangular cross-section, located across the flow in channel walls. If the cavity width is sufficient compared to its length along the flow, main characteristics of the flow at a sufficient distance from the side walls are well modeled in a two-dimensional approximation [1]. But under certain conditions, transversal instability can develop in the cavity, which leads to formation of three-dimensional structures, which in turn can affect the external flow behind the cavity [2, 3].

Large-scale elements of the flow structure in the vicinity of a cavity depend significantly by interaction of the shear layer formed from the local boundary layer shedding from the trench upper edge with the flow inside the cavity. Depending on the place of attachment of the shear layer, open and closed flow regimes are distinguished [4]. If the shear layer impinges upon the lower wall near its edge and one circulation zone is formed beneath (which is typical for the length-to-depth ratio $w/h < 6 \div 8$), such a cavern is called open. If the shear layer attaches to the bottom and two independent circulation domains are formed near the walls, the cavity is closed, such regime is observed at $w/h > 10 \div 15$. A cavity flow between these two types is considered transitional. Also, the cavity depth (h) determines the shapes and sizes of vortex formations throughout it when the ratio is $0.2 < h/w < 1$ [5,6].

In this paper, the flow about wide rectangular trenches is considered, in which the flow pattern corresponding to an open cavity is formed.

1 Problem Formulation

The flow features in the channel with a cavity (Fig. 1) are investigated at the following geometric parameters: L1 = 70 mm, H = 40 mm, L2 = 70 mm, W = 10 mm, h = 2.5÷10 mm, L = 280 mm.

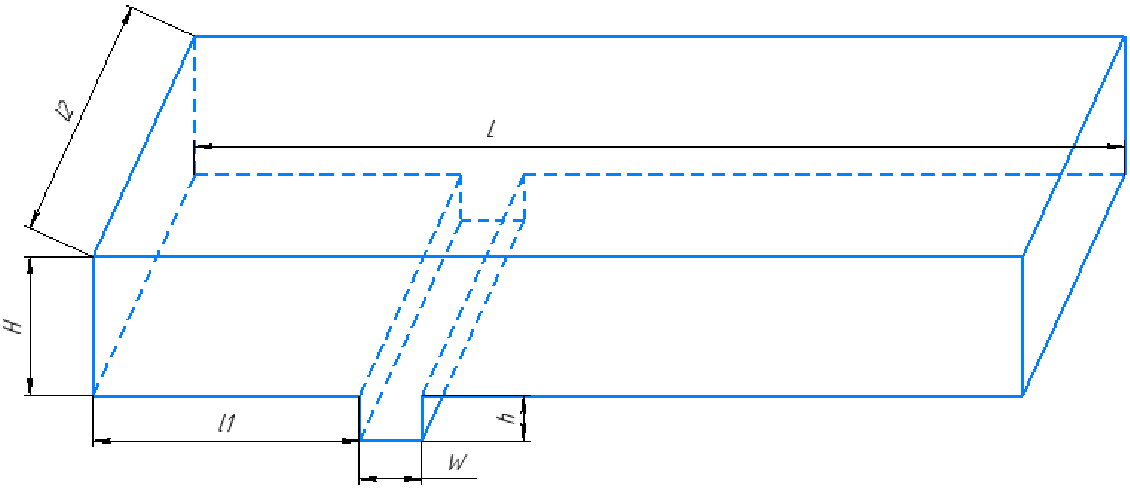

L1/L	0.26
H/h	4; 8; 16
L2/L	0.3
w/h	1; 2; 4
Rew	5000...10000
Red	25000...50000

Figure 1: The geometry of the researched domain

The mathematical model of the flow of a viscous incompressible fluid, which is used to solve this problem, includes (1-3):

- the momentum equation:

$$\rho\frac{\partial u_i}{\partial t}+\rho\frac{\partial\left(u_i u_j\right)}{\partial x_j}=-\frac{\partial p}{\partial x_i}+\frac{\partial}{\partial x_j}\left(\mu\left(\frac{\partial u_i}{\partial x_j}+\frac{\partial u_j}{\partial x_i}\right)\right), \qquad (1)$$

- continuity equation:

$$\frac{\partial u_j}{\partial x_j}=0, \qquad (2)$$

- energy equation:

$$\frac{\partial T}{\partial t}+u_j\frac{\partial T}{\partial x_j}=a\left(\frac{\partial^2 T}{\partial x_1^2}+\frac{\partial^2 T}{\partial x_2^2}+\frac{\partial^2 T}{\partial x_3^2}\right)+\frac{\mu}{2\rho Cp}\left(\frac{\partial u_i}{\partial x_j}+\frac{\partial u_j}{\partial x_i}\right)^2 \qquad (3)$$

To take into account the effect of the viscosity gradient on the flow stability, a polynomial describing the dependence of dynamic viscosity on temperature is introduced [8]:

$$\mu = 2,622\cdot 10^{-4}\cdot T^2-0,1783\cdot T+30,767\ \left[kg/(m\cdot s)\right].$$

The initial conditions of the problem correspond to the boundary conditions at the entrance to the channel.
Boundary conditions:
- the channel entrance: constant speed from the range of Reynolds numbers Re = 25000...50000, based on the channel hydraulic diameter and the wall temperature. The Reynolds number based on the trench length

in the flow direction (w), Re_w = 5000...10000. The temperature of the coolant at the entrance to the channel T_f = 333 K;
- channel walls: no-slip conditions and constant temperature T_w = 283 K;
- the channel exit: the Neumann boundary conditions for thermal and flow parameters.

The number of cells of the computational grid was about 6 million, with finer elements about walls and in the cavity (Fig.2). Since rather large-scale vortical structures are of interest in this study, strong constraints due to a grid are not critical.

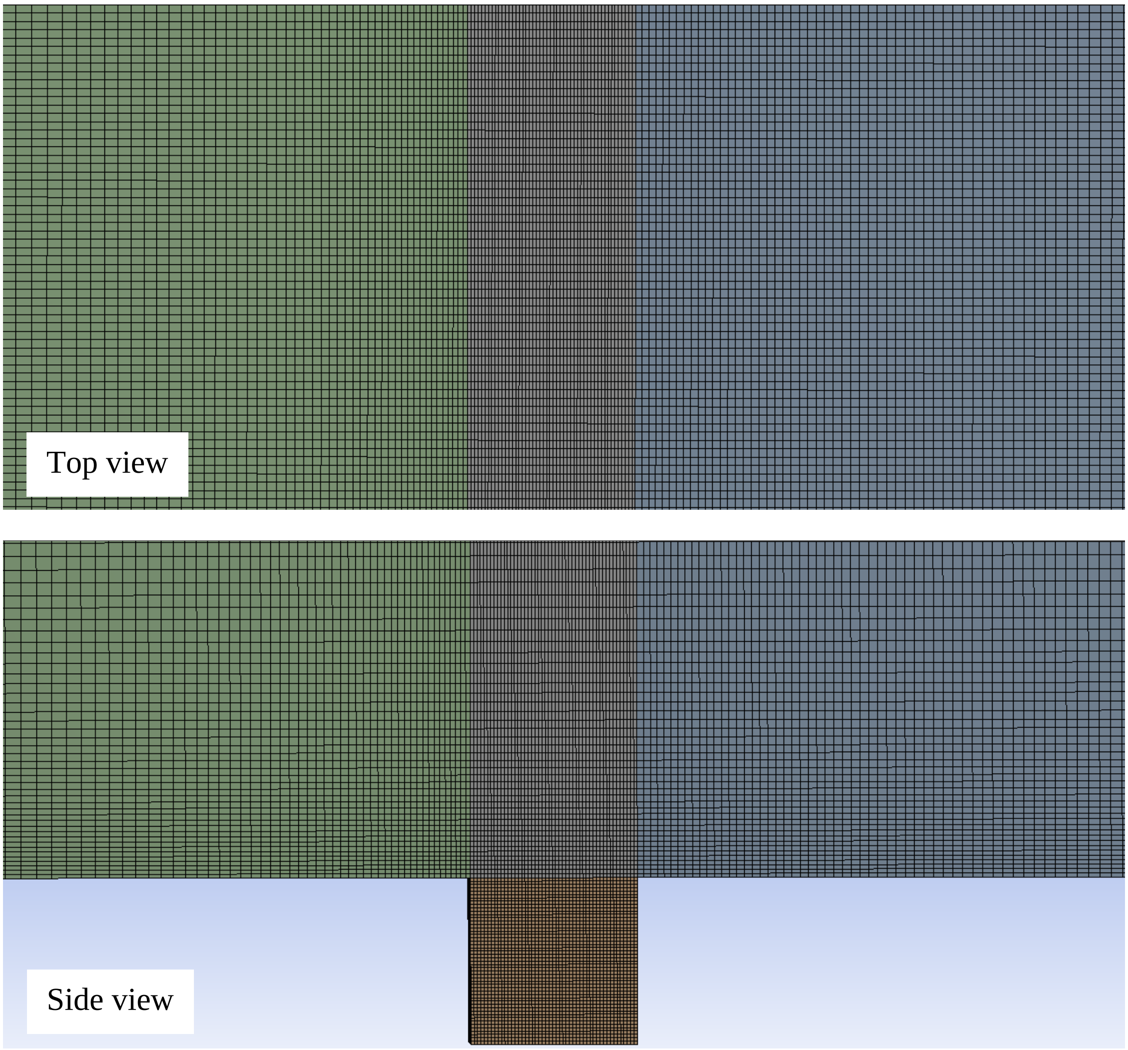

Figure 2: A fragment of the mesh

The time step was chosen in such a way as to minimize the computation time cost while fulfilling the Courant condition: Co =0.06 < 2.

In this study the finite volumes methods were used, with the segregated algorithm SIMPLEC to obtain the velocity and pressure fields (the basic equations are solved sequentially), the upstream scheme QUICK to discretize convective terms of the equations, first order implicit scheme for transient formulation.

2 Features of Vortex Structures inside the Cavity

Under the specified geometric dimensions and flow parameters, the cavity is placed in the initial section of the channel flow, when independent boundary layers are formed on walls, their thickness increases downstream. Its value at the cavity location is 1.75÷2 mm and close to the corresponding thickness in the smooth plate flow. At the same time, the ratio of the momentum thickness θ and the cavity length w does not exceed ~40. This value approaches the threshold value for the beginning of transition from a stationary

to an oscillatory regime in a two-dimensional cavity revealed in many studies of similar flows [1,6,7], when instantaneous parameters of the flow vary significantly in time.
In our case, a rather stable flow pattern is formed in the three-dimensional cavity with a shear layer that impinges onto the windward edge of the trench. Its lower part changes direction along the windward wall and forms a large vortex in its vicinity (Fig. 3).

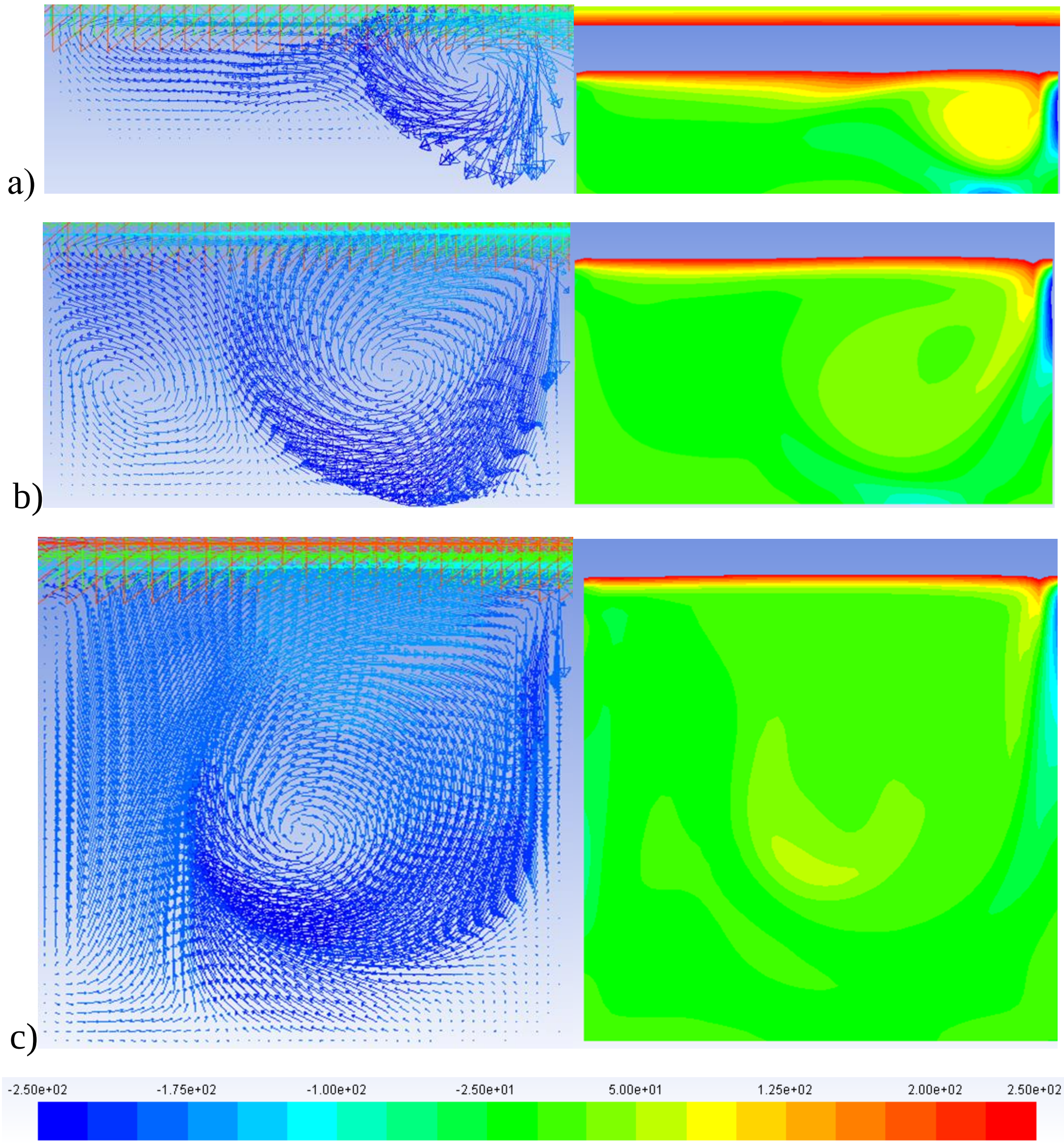

Figure 3: Velocity vector and transverse component of vorticity in the cavity cross section at Re = 25000, depending on depth: a) w/h = 4, б) w/h = 2, в) w/h = 1

The peculiarity of this vortex formation is, firstly, its stability for all studied geometric dimensions of the cavity and Reynolds numbers in the considered range. Secondly, this vortex is characterized by greatest intensity/vorticity (Fig. 3), therefore, it is the main energy-carrying vortex in the vortical system of the cavity. Thirdly, the scale of this vortex and the vorticity level are determined by the cavity depth, that is, diameter is proportional to depth. At the same speed of the external flow, the maximum vorticity in the cavity increases with decreasing depth, because the vortex inner part is solid-like rotating. An increase in the Reynolds number in the considered range naturally leads to an increase of vorticity, but it did not make a significant effect on stability and scale of the main vortex.

The vorticity fields allow us to make another observation about the nature of the shear layer and its interaction with inner and exrenal flows. Thus, with increasing Reynolds number low-amplitude oscillations of the shear layer appear in the vorticity field, which are more clearly seen at lower values of θ/w than in a two-dimensional case. On the other hand, the oscillation are more pronounced at a smaller depth of the cavity, where the outer flow had a greater effect on the inner region of the cavity.

Visualization of the flow inside the cavity showed that the flow is not uniform in the transverse direction. This is more evident in deeper cavities where, depending on the transverse coordinate, the vortex shape changes: it either expands occupying almost the entire cavity cross-section, or, on the contrary, shrinks leaving more space for formation of clearly visible secondary vortices (Fig. 4).

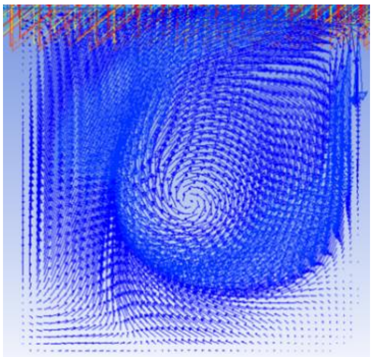

a)

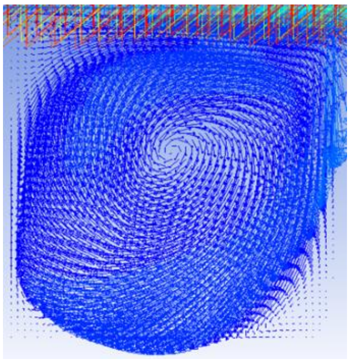

b)

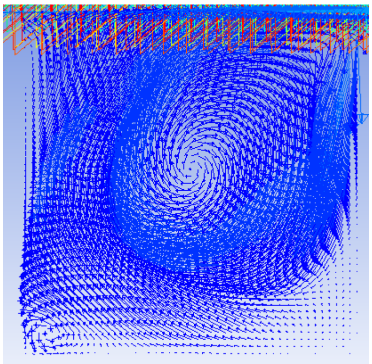

c)

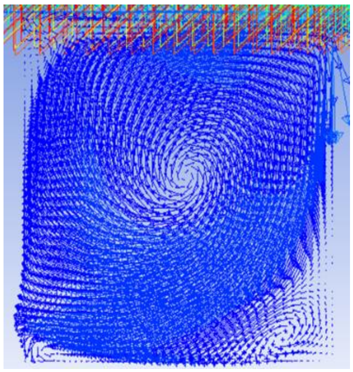

d)

Figure 4: Velocity vector field in different sections of the cavity w/h = 1 at Re = 25000 (a - y/L2 = 0.5, b - y/L2 = 0.528, c - y/L2 = 0.571, d - y/L2 = 0.6)

Observing time variations of the velocity vector fields in particular longitudinal sections, it can be noted that dimensions of the main vortex similarly vary in time. Its centres also move along a closed circular path. Thus, varicose shrinks and expansions move along the main vortex, which has the shape of almost round transverse filament (along the cavity span), and its axis performs oscillating movements in both horizontal and vertical directions. So, inside the cavity we observe a traveling transverse wave.

Now let's consider the features of the secondary transverse vortex structures, which are formed near the main vortex and redistribute the vortex motion energy inside the cavity. Usually their number is odd and their scales and shapes are determined by the cavity and main vortex dimensions. Depending on the cavity length-to-depth ratio, they can be elongated in horizontal (Fig. 3, a) or vertical directions (Fig. 3, c), or almost the same size as the main vortex (Fig. 3, b). They are weaker in terms of vorticity intensity but in a deeper cavity they manifest in characteristic spots in pressure fields on the leeward wall.

The fields of longitudinal vorticity on the windward wall have an intermittent structure in the transverse direction with maximum and minimum levels in the upper part (Fig. 5), which indicates the formation of vortex structures near this wall of the scale that corresponds to the transverse wave length. From Fig. 5, average dimensionless wavelength is ~0.075, so the cavity contains 13-14 vortex formations, the location of which is also reflected in the wavy shape of pressure fields on the windward wall (Fig. 6). Such structures are similar to those identified in [3] as Gortler-like vortices developing due to flow curvature in the main vortex. In the same manner, counter-rotating pairs are better discernible in the cavity with aspect ratio w/h = 1, where the main vortex occupies almost the entire cavity.

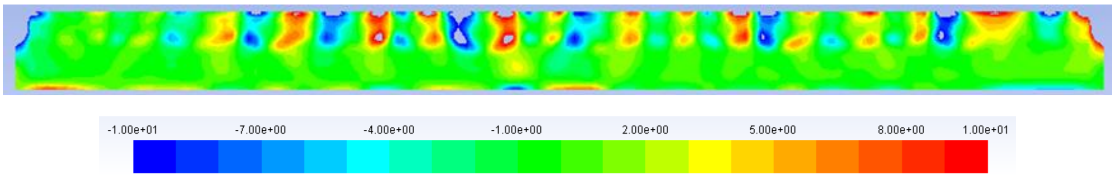

Figure 5: Longitudinal vorticity field on the windward wall of the cavity (flow direction from us) at Re = 25000 and w/h = 2

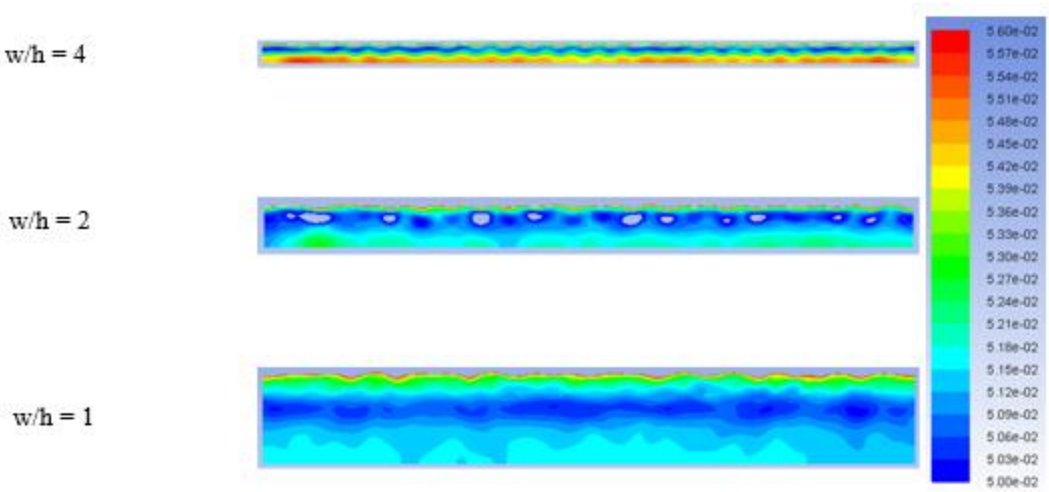

Figure 6: Pressure distribution on the windward sides of the cavity at Re = 25000

The considered features of the vortex flow determine the appropriate distribution of pressure on the cavity walls. In Fig. 6 we see layered vertically and heterogeneous horizontally pressure patterns on the windward sides of cavities with different depth. The highest pressure values are observed close to the edge, where the shear layer impinges upon the wall. Downward pressure decreases due to the main vortex and again rises to the bottom, for shallower cavities more.

Considering the pressure difference between the leeward and windward sides of the cavity, we can evaluate the pressure drag induced by the cavity in dependence on its shape and the Reynolds number. Thus, as the cavity depth increases and the main vortex area grows, that difference decreases, correspondingly decreases the cavity pressure drag (Fig. 7).

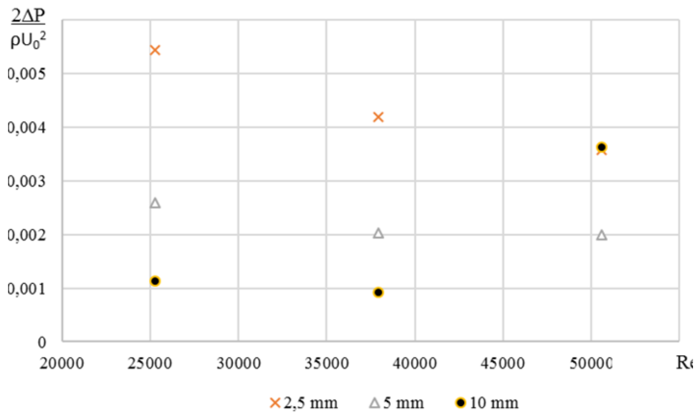

Figure 7: Pressure drag of the cavity depending on its depth

Although there is local rise of pressure over the cavity section in the channel wall, it does not lead to any significant alteration of its total drag.

Consider the influence of the vortex structure inside the cavity on the value of the wall shear stress. At the edges, where the thickness of the boundary layer is minimal, a local maximum of wall shear stress values is observed (Fig. 8). The presented plots show the dependence of friction drag coefficient on the

Reynolds number and the cavity depth. It becomes negative on the bottom with minimum below the main vortex, which intensifies as the cavity becomes shallower. Negative drag values in the cavity compensate its increases about edges, so overall friction drag of the wall section with the cavity is close to zero.

From the dimensionless wall shear stress plots, it is also seen that the cavity shape can affect the flow stability. Thus, at the greatest depth of the cavity, fluctuations in wall shear stress values appear closer to the channel outlet. This instability is better manifested for deeper cavities that corresponds to more transversally varied flow in the cavity and downstream, and at lower Reynolds number values when damping effect of viscosity is stronger in a thinner boundary layer. It can be said that the presence of a cavern provokes an earlier transition to a turbulent flow regime.

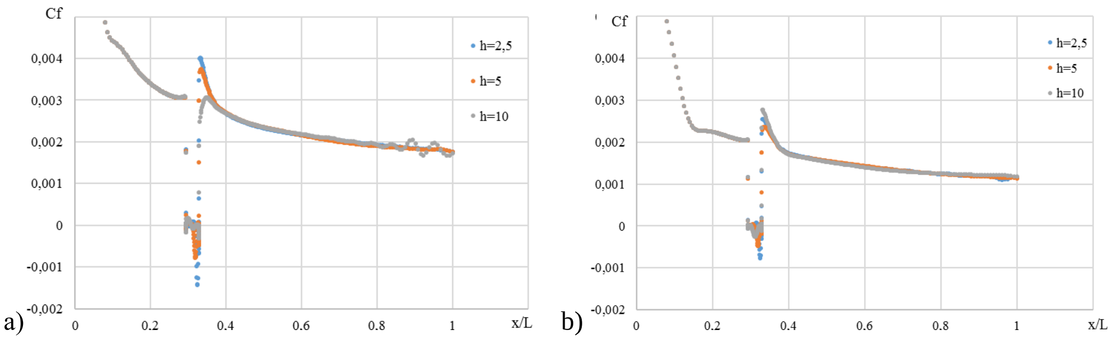

Figure 8: Friction drag coefficient in the cavity, depending on the Reynolds number:
a) Re = 25000, b) Re = 50000

The features of vortex structures also determine the intensity of heat transfer inside and outside the cavity. The highest values of heat transfer, like for wall shear stress, are observed at the downstream edge and behind, where the boundary layer is disturbed by vortical structures formed outside the cavity. The heat flux field inside the cavity has a more complex structure (Fig. 9).

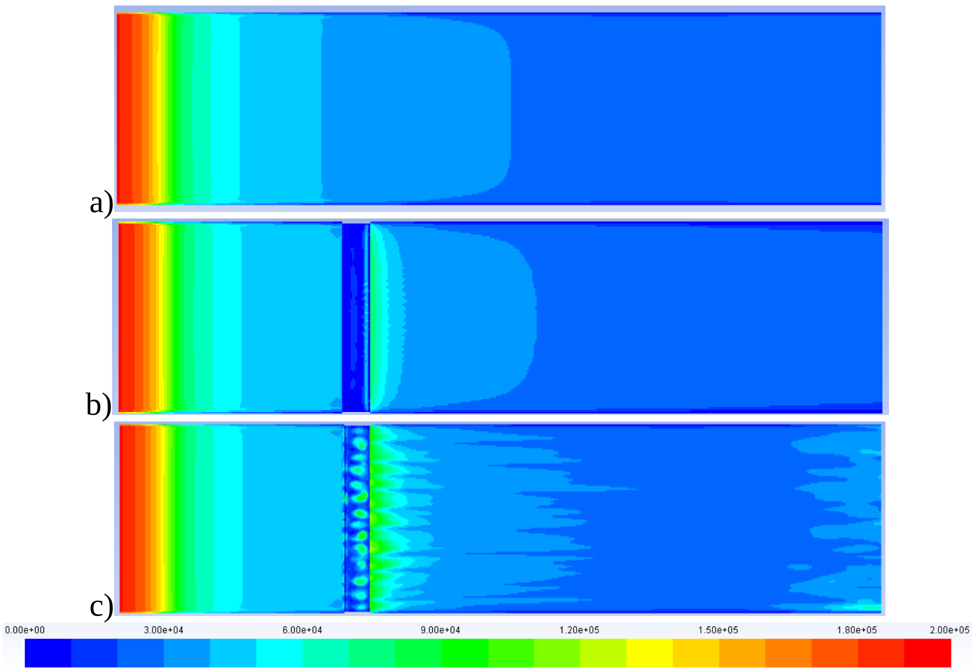

Figure 9: Heat flux density in the cavity, depending on its depth at Re = 25000:
a) smooth channel, b) w/h = 4, d) w/h = 1

The vortex structures inside do not interact so intensively with the external flow and do not provide intensive convective heat transfer between the internal and external flow because they are separated by the shear layer on most of the cavity length. However, local maxima of heat transfer are observed in places where the vortices touch the cavity walls and destroy boundary layers. This is observed in the deepest cavities among those considered.

At the analysed flow parameters, the vortex structures generated inside and outside the cavity have rather low intensity, so integral changes of heat transfer in the channel do not exceed 19%.

Conclusions

The flow in a three-dimensional cavity with side walls develops significant inhomogeneity of vortex motion in transverse direction over time even at moderate Reynolds number. It can lead to earlier occurrence of flow instability than can be obtained in the frame of two-dimensional approach. In a cavity with the aspect ratio ~1 the transversal instability is most manifested in development of longitudinal secondary vortices near the cavity walls, which can be considered as Gortler-like vortices. Correspondingly, it generates transversal variations of flow parameters downstream the cavity and can lead to earlier development of the external flow instability.

References

[1] Yoshida, T. & Watanabe, T.: Numerical Simulation of Flow over an Open Cavity with Self-Sustained Oscillation Mode Switching. *Open Journal of Fluid Dynamics*, vol 6, (2016) pp. 361-370.http://dx.doi.org/10.4236/ojfd.2016.64027

[2] Brès, G. & Colonius, T.: Three-dimensional instabilities in compressible flow over open cavities. *Journal of Fluid Mechanics*., vol. 599, (2008) pp. 309-339.

[3] Faure, T.M., Adrianos, P., Lusseyran, F. & Pastur, L.: Visualizations of the flow inside an open cavity at medium range Reynolds numbers. *Exp Fluids*, vol. 42, (2007) pp. 169–184. https://doi.org/10.1007/s00348-006-0188-8

[4] Debiasi, M.: Experimental Exploration of Cavity Flow Physics, Retrieved from http://www.marcodebiasi.net 2011.

[5] Belinskiy, V.G., Voropayev, G.A., Voskoboynik, A.V., Paramonov, YU. A.: Eksperimental'noye issledovaniye soprotivleniya i kartiny obtekaniya pryamougol'nykh kavern v turbulentnom potoke. *Prikladna gidromekhanika*. vol. 14, №4. (2012) pp. 3-25

[6] Rozumnyuk, N. V.: Mgnovennyye i osrednennyye kharakteristiki vyazkogo potoka okolo pryamougol'noy kaverny. *Prikladna gidromekhanika*. vol. 9(81), N 4. (2007) pp. 49–58

[7] Knisely, C., Rockwell, D.: Self-Sustained Low-Frequency Components in an Impinging Shear Layer. *Journal of Fluid Mechanics*, 116 (1982), 157-186.

[8] Rivkin, S. L., Aleksandrov, A. A.: Thermodynamic Properties of Water and Water Vapor: Handbook. Recommended by the State Service for Standard Reference Data – 2nd Edition, Revised and Supplemented. Moscow: Energoatomizdat, 1984. 80 pages. (in Russian)